ARL-TR-10448 ● Sep 2026

Effects of Agitation-Induced Shear Stress on *Curvularia lunata* Branching Morphology

by Kelsey Gray, Jordan Baumbach, Matthew Servinsky, and Bryn Adams

NOTICES

Disclaimers

The findings in this report are not to be construed as an official Department of the Army position unless so designated by other authorized documents.

Citation of manufacturer's or trade names does not constitute an official endorsement or approval of the use thereof.

Destroy this report when it is no longer needed. Do not return it to the originator.

ARL-TR-10448 ● Sep 2026

Effects of Agitation-Induced Shear Stress on *Curvularia lunata* Branching Morphology

Kelsey Gray
Oak Ridge Associated Universities, Postdoctoral Fellowship
DoD SMART Scholarship

Jordan Baumbach, Matthew Servinsky, and Bryn Adams
DEVCOM Army Research Laboratory

REPORT DOCUMENTATION PAGE

1. REPORT DATE	2. REPORT TYPE	3. DATES COVERED	
		START DATE	END DATE
September 2026	Technical Report	17 February 2026	18 May 2026

4. TITLE AND SUBTITLE
Effects of Agitation-Induced Shear Stress on *Curvularia lunata* Branching Morphology

5a. CONTRACT NUMBER	5b. GRANT NUMBER	5c. PROGRAM ELEMENT NUMBER
5d. PROJECT NUMBER	**5e. TASK NUMBER**	**5f. WORK UNIT NUMBER**

6. AUTHOR(S)
Kelsey Gray, Jordan Baumbach, Matthew Servinsky, and Bryn Adams

7. PERFORMING ORGANIZATION NAME(S) AND ADDRESS(ES)
DEVCOM Army Research Laboratory
ATTN: FCDD-RLA-MI
Adelphi, MD 20783

8. PERFORMING ORGANIZATION REPORT NUMBER
ARL-TR-10448

9. SPONSORING/MONITORING AGENCY NAME(S) AND ADDRESS(ES)	10. SPONSOR/MONITOR'S ACRONYM(S)	11. SPONSOR/MONITOR'S REPORT NUMBER(S)

12. DISTRIBUTION/AVAILABILITY STATEMENT
DISTRIBUTION STATEMENT A. Approved for public release: distribution unlimited.

13. SUPPLEMENTARY NOTES
ORCIDs: Kelsey Gray, 0000-0003-2940-1476; Jordan Baumbach, 0009-0004-9051-6453; Matthew Servinsky, 0005-0045-1787-2407; Bryn Adams, 0000-0001-8009-2133

14. ABSTRACT
This study investigates the morphological control of the melanin-producing fungus *Curvularia lunata* to support the development of melanized biomaterials for advanced military applications. While researchers seek to dictate morphology using agitation-induced shear stress, the quantitative relationships governing these dynamics remain poorly characterized. *C. lunata* was cultivated across various agitation speeds (50–250 rpm), flask sizes (250 and 500 mL), and media volumes to further tease out the impact of differences in agitation-induced shear stress. However, efforts to isolate and magnify these mechanical differences revealed that shear stress cannot be separated from the broader physiochemical system. The results demonstrate that while massive differences in agitation drive a distinct hyperbranching response, the dominating influence of agitation-induced shear stress on morphological outcomes is reduced at lower speeds. As agitation becomes less overwhelming, inseparable environmental variables—coupled with the fungus's own biological responses—predominate. Specifically, these lower-shear environments promoted the secretion of extracellular polysaccharides, driving hyphal aggregation and subsequent anastomosis (hyphal fusion). Ultimately, our findings show that morphological control cannot be reduced to stirring intensity alone; rather, it requires a systemic approach that accounts for both network expansion and network connection mechanisms.

15. SUBJECT TERMS
melanized biomaterials, *Curvularia lunata*, agitation-induced shear stress, extracellular polysaccharides, EPS, shear-induced morphogenesis, anastomosis, hyphal fusion, morphological control, non-model fungi, Biological and Biotechnology Sciences

16. SECURITY CLASSIFICATION OF:			17. LIMITATION OF ABSTRACT	18. NUMBER OF PAGES
a. REPORT	b. ABSTRACT	C. THIS PAGE		
UNCLASSIFIED	UNCLASSIFIED	UNCLASSIFIED	UU	23

19a. NAME OF RESPONSIBLE PERSON	19b. PHONE NUMBER *(Include area code)*
Bryn Adams	(520) 691-6330

STANDARD FORM 298 (REV. 5/2020)
Prescribed by ANSI Std. Z39.18

Contents

List of Figures

1. Introduction

The development of melanized biomaterials is of significant interest to the U.S. Army for potential integration into advanced Warfighter equipment. Melanin, a highly valued natural biopolymer, is prominently found in filamentous fungi—organisms characterized by root-like structures called hyphae that branch to form resilient networks known as mycelia.[1–5] These fungi are widely recognized as formidable biomaterials due to their structural strength and ability to grow rapidly using minimal inputs.[6–10] However, to successfully harness and incorporate these melanized biomaterials into Army applications, precise control over their branching morphology, or appearance, is essential. Currently, mechanisms to reliably dictate these morphological outcomes remain an active area of research.

The expansion of fungal networks is determined by two primary physical behaviors: exploratory growth (apical elongation and lateral branching) and network connection (hyphal aggregation and anastomosis/hyphal fusion).[11–16] Research reports numerous environmental cues largely influence these expansion behaviors, but anastomosis, or the physical fusion of neighboring hyphae to form connected networks known as hyphal fusion, often obscures more mature mycelial networks and complicates research efforts to characterize the impacts of individual environmental variables.[11,13,17,18] This limitation drives most research to focus on controlling space-filling behaviors through the manipulation of growth environments such as changing agitation speeds.[19] Morphological outcomes from these studies are species dependent, demonstrating a need for dedicated characterization of non-model organisms.[20–24]

This study investigates *Curvularia lunata*, a highly melanated fungus of interest, and its morphological response to agitation-induced shear stress. This work was motivated by Dr. Matthew Servinsky's preliminary observations of *C. lunata*'s disparate morphologies under two different extremes of agitation-induced shear stress. To better understand *C. lunata* morphologies for material generation, this work utilizes a novel quantitative characterization between agitation-induced shear stress and hyphal branches in a shaking incubator.

2. Methods and Procedures

2.1 Fungal Strains and Growth Media

In all experiments, we used the 42011 wild-type strain of *C. lunata* obtained from the American Type Culture Collection (ATCC, Manassas, Virginia) and grown on Potato Dextrose Agar (PDA) agar plates until confluency.

2.2 Preparation of Samples in 250-mL Shake Flask

Conidia from confluent PDA plates of *C. lunata* were harvested using 5 mL of sterile deionized (DI) water and a sterile L-shaped cell spreader. Spore solution was filtered through a 40-µm cell strainer (Greiner Biosciences) and diluted to a concentration of 4,000 conidia/mL. The diluted solution was inoculated into 250-mL unbaffled glass volumetric flasks containing 100 mL of yeast peptone dextrose (YPD) liquid media. Inoculated flasks were shaken at a single speed for 15.5 h at 28 °C. The speeds tested were 50, 125, and 250 rpm, and three different bioreplicates were used for each speed.

2.3 Preparation of Samples in 500-mL Shake Flask

Conidia from confluent PDA plates of *C. lunata* were harvested using 5 mL of sterile DI water and a sterile L-shaped cell spreader. Spore solution was filtered through a 40-µm cell strainer and diluted to a concentration of 4,000 conidia/mL. The diluted solution was inoculated into 500-mL unbaffled glass volumetric flasks containing 100 mL of YPD liquid media. Inoculated flasks were shaken at a single speed for 15.5 h at 28 °C. The speeds tested were 50, 75, 100, and 125 rpm, and three different bioreplicates were used for each speed.

2.4 Preparation of Samples in 500-mL Shake Flask in 60 mL of YPD

Conidia from confluent PDA plates of *C. lunata* were harvested using 5 mL of sterile DI water and a sterile L-shaped cell spreader. Spore solution was filtered through a 40-µm cell strainer and diluted to a concentration of 4,000 conidia/mL. The diluted solution was inoculated into 500-mL unbaffled glass volumetric flasks containing 60 mL of YPD liquid media. Inoculated flasks were shaken at a single speed for 15.5 h at 28 °C. The speeds tested were 75 and 100 rpm, and three different bioreplicates were used for each speed.

2.5 Imaging of Fungal Hyphae

To image hyphae for branching analysis, shake flasks were removed from the incubator after 15.5 h, gently scraped with an autoclaved plastic spatula, swirled to collect all the loose hyphae in the flask, and emptied into 500-mL Nalgene filter units. While gently swirling the Nalgene unit, the liquid is filtered through with a vacuum on low to isolate the hyphae. While the vacuum is off, 10 mL of sterile DI water is added back to the top of the Nalgene unit, gently scraped with a new plastic spatula, swirled again, and emptied into a 50-mL conical tube. After using the number “2” setting to vortex the spore solution in the conical tube for 7 s, a p100

micropipette with a diagonal cut at the second hash mark of the p100 tip was used to aspirate 25 µL of spore solution onto a microscope slide. After covering the microscope slide, 40 images—identifying at least 1 hyphae clearly—were taken using an inverted microscope at 10× magnification (Mateo FL) under brightfield and contrast lenses.

2.6 Analysis of Fungal Hyphae

For each bioreplicate, the number of tips for 30 different hyphae analyzed from the images collected were counted and placed on a spreadsheet. The total number of hyphal tips, representing branching, was averaged per condition (agitation speed, volume of shake flask, and volume of media) and graphed along with their respective standard error for comparison.

3. Results and Discussion

3.1 Branching Analysis of 250-mL Shake Flask Samples

Previous studies show that fungal branching is a dynamic response to its environment.[25–28] Our original hypothesis, inspired by Dr. Servinsky's early observations, anticipated that environments with greater agitation-induced shear stress would increase both hyphal collision frequency and local oxygenation—two synergistic factors that change the local environment and are suspected to drive enhanced hyphal branching.[26,29–35] Figure 1 shows samples grown at 50, 125, and 250 rpm. Figure 2 shows samples grown at 250 rpm exhibited a significantly higher average number of hyphal tips ($P < 0.05$) compared to those grown at 50 and 125 rpm. No significant difference was observed between 50 and 125 rpm despite a twofold difference in speed. Although the 250-rpm data demonstrates that doubling the agitation rate can drive a distinct branching response, the lack of variation between the lower speeds exhibiting a similar twofold difference suggests that the current growth environment may obscure the authentic branching morphologies we expected at lower agitation thresholds.

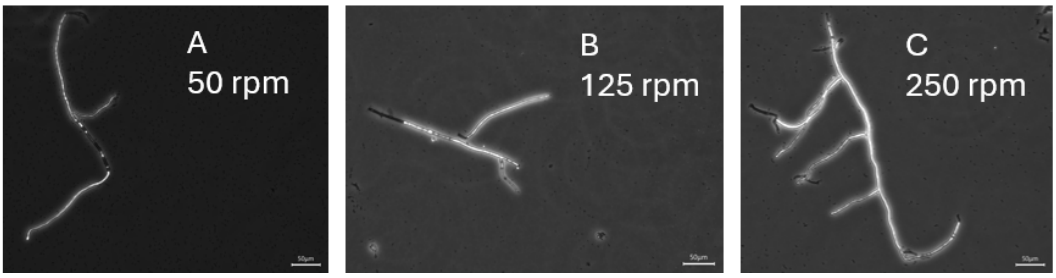

Figure 1. Representative images of samples grown at (A) 50, (B) 125, and (C) 250 rpm within 250-mL shake flask taken with a light microscope. Size bars = 50 µm.

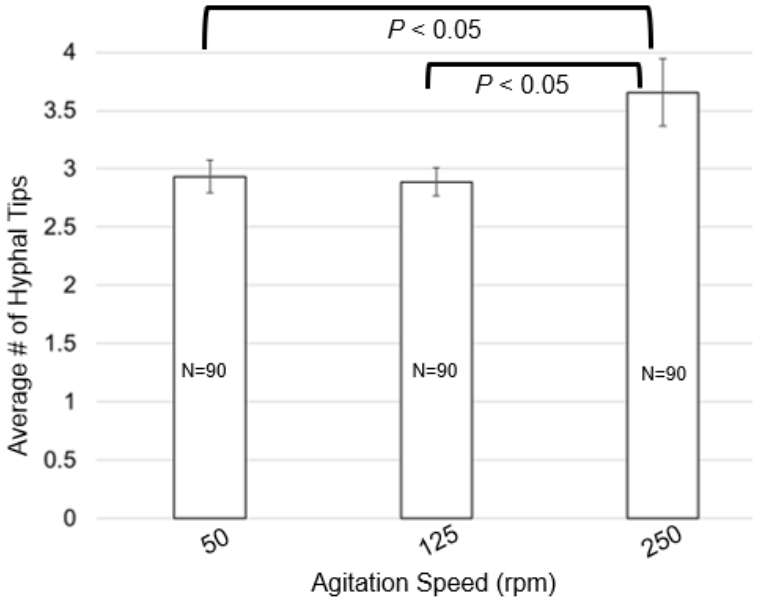

Figure 2. Average number of hyphal tips for samples grown in 250-mL shake flask at agitation speeds of 50, 125, and 250 rpm for 15.5 h. Samples grown at 250 rpm exhibit significantly more hyphal tips compared to samples grown at 50 and 125 rpm. Error bars indicate standard error of mean.

3.2 Branching Analysis of 500-mL Shake Flask Samples

To more accurately assess the relationship between agitation-induced shear stress and resulting branching morphologies, we reduced oxygen and nutrient gradients suspected of obscuring differences between agitation speeds in the previous environment by repeating the experiment at 50, 75, 100, and 125 rpm within a larger 500-mL glass, unbaffled shake flask containing 100 mL of media. Figure 3 shows that samples grown at 125 rpm have significantly more hyphal tips compared to samples grown at 50 and 75 rpm. Samples grown at 100 rpm statistically produce an equal amounts of hyphal tips compared to samples grown at 50, 75, and 125 rpm, suggesting that a critical energy threshold—greater than the energy produced at 100 rpm in this environment—is required to significantly alter hyphal branching.[20,36–41] Similar studies report that energy thresholds are governed by shear stress, which is naturally inseparable from other physiochemical variables—mainly including mass transfer rates and fluid dynamics.[41–43] Therefore, altering the agitation speed simultaneously impacts multiple variables within a shake flask, inducing a systemic change across the entire growth environment.

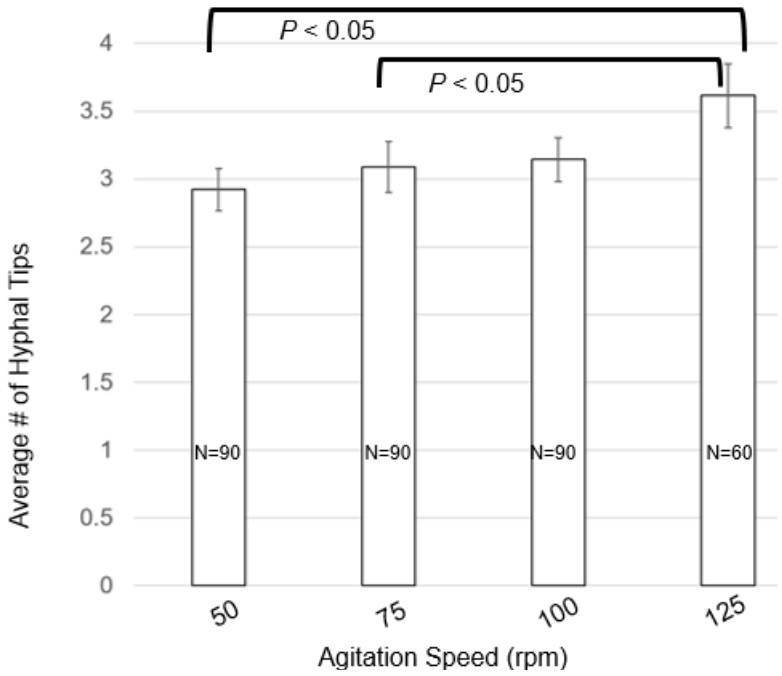

Figure 3. Average number of hyphal tips for samples grown in 500-mL shake flask at agitation speeds of 50, 75, 100, and 125 rpm for 15.5 h. Samples grown at 125 rpm exhibit significantly more hyphal tips compared to samples grown at 50 and 75 rpm. Error bars indicate standard error of mean.

Figure 4 illustrates how different environments—one inside a 500-mL shake flask operating at a 20% fill ratio and the other inside a 250-mL shake flask operating at a 40% fill ratio—alter hyphal branching outcomes at 50 and 125 rpm across identical initial conditions. Our data shows samples grown in 500-mL shake flasks at 125 rpm exhibit significantly more hyphal tips than samples grown in 250-mL shake flasks; samples grown at 50 rpm exhibited identical hyphal branching tip averages in both vessels. Flask volume-induced environmental differences affected branching at 125 rpm as predicted but not at 50 rpm, suggesting a low speed created a quasi-static growth environment at 50 rpm that was outside the scope of this study.

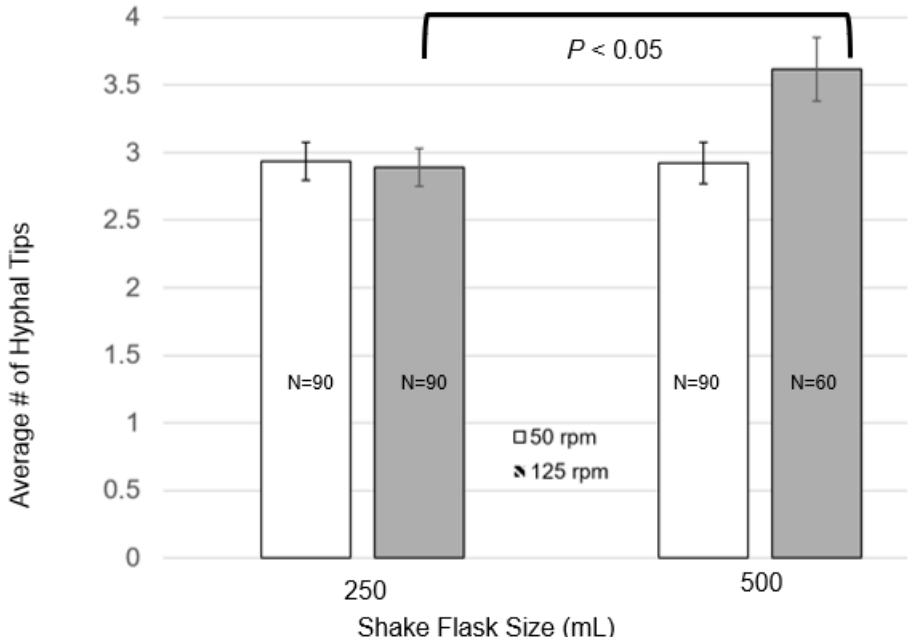

Figure 4. Comparison of average number of hyphal tips between samples of the same speed grown in different sizes of shake flasks. The average number of tips is significantly different between samples grown at 125 rpm in different sizes of flasks, but this is not different for samples grown at 50 rpm, which indicates that 50 rpm is inadequate for evaluating agitation-induced shear stress effects on hyphal branching.

3.3 Branching Analysis of 500-mL Shake Flask Samples in 60 mL of YPD

To better characterize how agitation-induced shear stress impacts branching morphologies, we repeated the previous experiments using 60 mL of media in 500-mL shake flasks at 75 and 100 rpm. We hypothesized the reduced volume of media would further mitigate both oxygen and nutrient gradients suspected of obscuring differences between agitation speeds from previous conditions. We expected this change would magnify differences in hyphal branching between speeds. Figure 5 shows a significant decrease in branching among the samples grown in 60 mL of media compared to the samples grown in 100 mL, but there was no difference in hyphal branching between different speeds grown in the same volume of media.

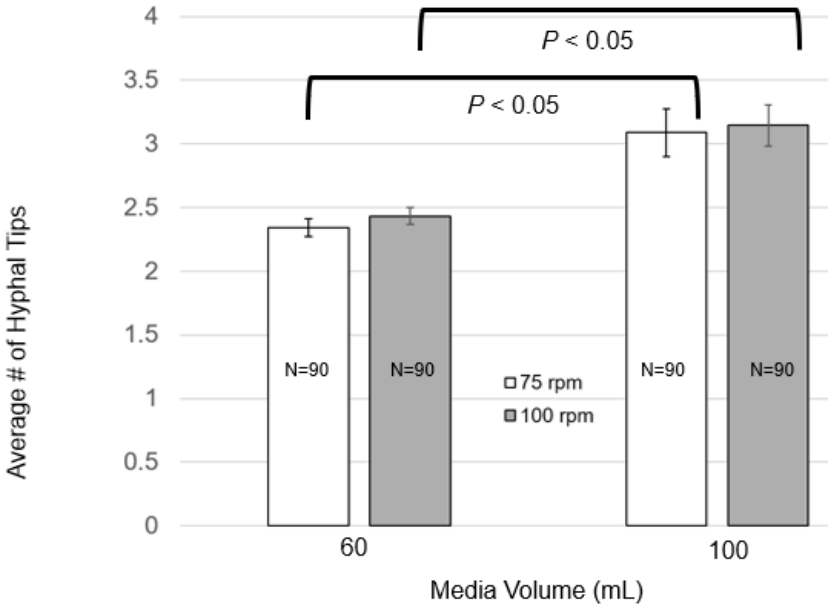

Figure 5. Comparison of the average number of hyphal tips between samples of the same speed grown within the same size of shake flasks containing different volumes of media. The average number of tips is significantly lower between samples grown in 60 mL of media compared to samples grown in 100 mL of media.

The identical branching morphologies consistently observed across different environments within a narrower range of agitation speeds suggest that other variables besides shear stress may significantly influence morphological outcomes. In addition, all shake flasks containing 60 mL exhibited reduced branching compared to their 100 mL counterparts, contradicting previous trends of increased shear stress driving hyperbranching morphologies as observed in Figures 2 and 3. To identify the variables overriding the expected difference in branching from agitation-based shear stress, we examined the hyphal microenvironment. As shown in Figure 6A, we observed an abundance of suspected extracellular polysaccharides (EPS)—primary contributors to the aggregation of hyphae[44–49] and known precursors to anastomosis capable of altering late-stage fungal morphology.[13,18,50–52] The EPS in Figure 6A was visually identified based on its characteristic mucous-like appearance surrounding the hyphae, consistent with morphological descriptions and imaging standards established in literature.[53–57]

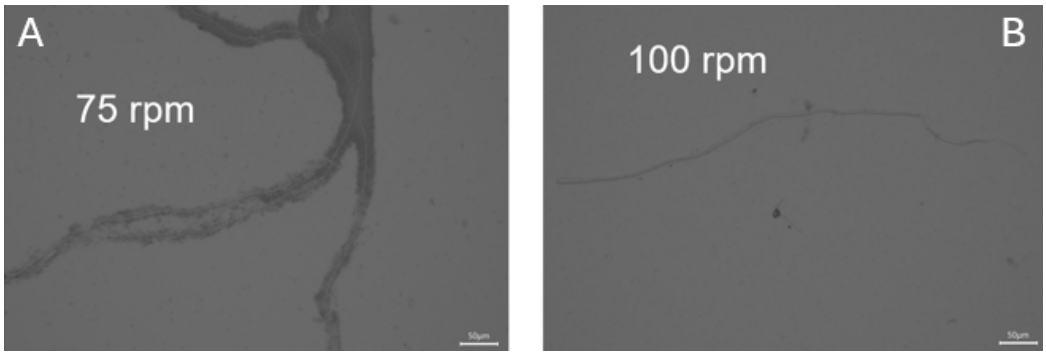

Figure 6. Samples grown in 60-mL samples within 500-mL shake flask at different speeds. Panel A shows an abundance of extracellular polysaccharides secreted by the hyphae surrounding its perimeter, whereas panel B shows minimal presence of the EPS collecting around the hyphae at a higher speed.

4. Conclusions

In the fungal manufacturing industry, specific morphologies are known for driving the bioprocessing of high-value products.[26] A complete understanding of 1) critical process parameters, 2) how these processes can be controlled, and 3) resulting fungal morphologies are required for maximizing the industrial potential of fungi as a living production platform.[26] The same logic should be applied for the successful use of fungi as a living material concerning Army applications. This study investigates a quantitative characterization of the relationship between agitation-induced shear stress—a critical process parameter—and representative branching dynamics in *C. lunata* within nutrient-abundant shake flask environments.

Researchers' current efforts to understand the morphological control of fungi largely consist of species-dependent results accrediting morphology exclusively to agitation rates but overlooking how stirring alters the entire physiochemical system.[11,12,58–60] Our findings demonstrate that massive differences in agitation-induced shear stress drive a hyperbranching response while also indicating the existence of a potential critical energy threshold. Our data shows when agitation intensity decreases towards a critical energy threshold that typically induces hyperbranching responses within an environment, the inseparable variables accompanying agitation and the fungus's own secondary biological responses gain more influence over the organism's final morphology. Specifically, at these lower agitation speeds, we observed a collection of EPS from *C. lunata* that we suspect led to anastomosis (hyphal fusion) based on our data.[13,18,50–57]

Improved control of morphological outcomes requires deeper knowledge of how an entire system responds to input changes such as agitation speed. Further studies of anastomosis, particularly in relation to EPS production within production

vessels, are the recommended next steps to accomplish this. Combining this effort with continued studies of associated parameters, such as nutrient gradients and oxygen transfer rates, will lead to a comprehensive understanding of the relationship between shear stress and morphology necessary for improved material generation and expanded application use.

5. References

1. Chongkae S et al. Production of melanin pigments in saprophytic fungi in vitro and during infection. Journal of Basic Microbiology. 2019;59(11):1092–1104.
2. Eisenman HC, Casadevall A. Synthesis and assembly of fungal melanin. Applied Microbiology and Biotechnology. 2012;93(3):931–940.
3. Pihet M et al. Melanin is an essential component for the integrity of the cell wall of *Aspergillus fumigatus* conidia. BMC Microbiology. 2009;9(1):177.
4. Pombeiro-Sponchiado SR, Sousa GS, Andrade JC, Lisboa HF, Gonçalves RC. Production of melanin pigment by fungi and its biotechnological applications. Melanin. 2017;1(4):47–75.
5. Suthar M, Dufossé L, Singh SK. The enigmatic world of fungal melanin: a comprehensive review. Journal of Fungi. 2023;9(9):891.
6. Appels FVW et al. Fabrication factors influencing mechanical, moisture-and water-related properties of mycelium-based composites. Materials & Design. 2019;161:64–71.
7. Elsacker E, Vandelook S, Peeters E. Recent technological innovations in mycelium materials as leather substitutes: a patent review. Frontiers in Bioengineering and Biotechnology. 2023;11:1204861.
8. Hinneburg H, Gu S, Naseri G. Fungal innovations—advancing sustainable materials, genetics, and applications for industry. Journal of Fungi. 2025;11(10):721.
9. Islam MR, Tudryn G, Bucinell R, Schadler L, Picu RC. Morphology and mechanics of fungal mycelium. Scientific Reports. 2017;7(1):13070.
10. Madusanka C et al. A review of recent advances in fungal mycelium based composites. Discover Materials. 2024;4(1):13.
11. Harris SD. Branching of fungal hyphae: regulation, mechanisms and comparison with other branching systems. Mycologia. 2008;100(6):823–832.
12. Harris SD. Hyphal branching in filamentous fungi. Developmental Biology. 2019;451(1):35–39.
13. Dikec J et al. Hyphal network whole field imaging allows for accurate estimation of anastomosis rates and branching dynamics of the filamentous fungus *Podospora anserina*. Scientific Reports. 2020;10(1):3131.

14. Richter F, Calonne-Salmon M, van der Heijden MGA, Declerck S, Stanley CE. AMF-SporeChip provides new insights into arbuscular mycorrhizal fungal asymbiotic hyphal growth dynamics at the cellular level. Lab on a Chip. 2024;24(7):1930–1946. https://doi.org/10.1039/d3lc00859b

15. Ledoux C et al. Prediction and experimental evidence of different growth phases of the *Podospora anserina* hyphal network. Scientific Reports. 2023;13(1):8501. https://doi.org/10.1038/s41598-023-35327-w

16. De La Providencia IE, De Souza FA, Fernández F, Delmas NS, Declerck S. Arbuscular mycorrhizal fungi reveal distinct patterns of anastomosis formation and hyphal healing mechanisms between different phylogenic groups. New Phytologist. 2005;165(1):261–271. https://doi.org/10.1111/j.1469-8137.2004.01236.x

17. Glass NL, Jacobson DJ, Shiu PKT. The genetics of hyphal fusion and vegetative incompatibility in filamentous ascomycete fungi. Annual Review of Genetics. 2000;34:165–186. https://doi.org/10.1146/annurev.genet.34.1.165

18. Francisco CS, Zwyssig MM, Palma-Guerrero J. The role of vegetative cell fusions in the development and asexual reproduction of the wheat fungal pathogen Zymoseptoria tritici. BMC Biology. 2020;18(1):99.

19. Krull R et al. Characterization and control of fungal morphology for improved production performance in biotechnology. Journal of Biotechnology. 2013;163(2):112–123. https://doi.org/10.1016/j.jbiotec.2012.06.024

20. El-Enshasy H, Kleine J, Rinas U. Agitation effects on morphology and protein productive fractions of filamentous and pelleted growth forms of recombinant *Aspergillus niger*. Process Biochemistry. 2006;41(10):2103–2112.

21. Johansen CL, Coolen L, Hunik JH. Influence of morphology on product formation in *Aspergillus awamori* during submerged fermentations. Biotechnology Progress. 1998;14(2):233–240.

22. Veiter L, Rajamanickam V, Herwig C. The filamentous fungal pellet—relationship between morphology and productivity. Applied Microbiology and Biotechnology. 2018;102(7):2997–3006.

23. Yanli Y, Xiaoyu Z, Hongxun W, Huiyan H. Effects of growth and producing laccase on *Pleurotus* by different shake flask conditions. Shengwu Jishu Biotechnology. 2004;14(5):72–76.

24. Cairns TC, Zheng X, Zheng P, Sun J, Meyer V. Moulding the mould: understanding and reprogramming filamentous fungal growth and morphogenesis for next generation cell factories. Biotechnology for Biofuels. 2019;12(1):77.

25. Kornitzer D. Regulation of *Candida albicans* hyphal morphogenesis by endogenous signals. Journal of Fungi. 2019;5(1):21.

26. Li Q et al. Morphological regulation of filamentous fungi improves industrial production. Biotechnology Advances. 2025:108793.

27. Ramírez-Sotelo U, Gómez-Gaviria M, Mora-Montes HM. Signaling pathways regulating dimorphism in medically relevant fungal species. Pathogens. 2025;14(4):350.

28. Schmieder SS et al. Bidirectional propagation of signals and nutrients in fungal networks via specialized hyphae. Current Biology. 2019;29(2):217–228.

29. Garcia-Ochoa F, Gomez E, Santos VE. Fluid dynamic conditions and oxygen availability effects on microbial cultures in STBR: an overview. Biochemical Engineering Journal. 2020;164:107803.

30. Kelly S, Grimm LH, Bendig C, Hempel DC, Krull R. Effects of fluid dynamic induced shear stress on fungal growth and morphology. Process Biochemistry. 2006;41(10):2113–2117.

31. Li C et al. CFD analysis of the turbulent flow in baffled shake flasks. Biochemical Engineering Journal. 2013;70:140–150.

32. Mancilla E et al. A hydrodynamic description of the flow behavior in shaken flasks. Biochemical Engineering Journal. 2015;99:61–66.

33. Palacios-Morales C et al. The flow inside shaking flasks and its implication for mycelial cultures. Chemical Engineering Science. 2016;152:163–171.

34. Serrano-Carreón L, Galindo E, Rocha-Valadéz JA, Holguín-Salas A, Corkidi G. Hydrodynamics, fungal physiology, and morphology. Filaments in Bioprocesses. 2015:55–90.

35. Xia X, Lin S, Xia XX, Cong FS, Zhong JJ. Significance of agitation-induced shear stress on mycelium morphology and lavendamycin production by engineered *Streptomyces flocculus*. Applied Microbiology and Biotechnology. 2014;98(10):4399–4407.

36. Serrano-Carreón L, Galindo E, Rocha-Valadéz JA, Holguín-Salas A, Corkidi G. Hydrodynamics, fungal physiology, and morphology. In: Krull R, Bley T, editors. Filaments in bioprocesses. Springer International Publishing; 2015. p. 55–90.

37. Brauneck G et al. Scale-up of *Streptomyces* species cultivations based on the morphological response to the energy dissipation rate. AIChE Journal. 2026;72(7):e70348.

38. Lu H et al. Dependence of fungal characteristics on seed morphology and shear stress in bioreactors. Bioprocess and Biosystems Engineering. 2015;38(5): 917–928.

39. Veiter L, Kager J, Herwig C. Optimal process design space to ensure maximum viability and productivity in *Penicillium chrysogenum* pellets during fed-batch cultivations through morphological and physiological control. Microbial Cell Factories. 2020;19(1):33.

40. Cui YQ, Van der Lans R, Luyben KCAM. Effect of agitation intensities on fungal morphology of submerged fermentation. Biotechnology and Bioengineering. 1997;55(5):715–726.

41. Cui YQ, Van der Lans R, Luyben KCAM. Effects of dissolved oxygen tension and mechanical forces on fungal morphology in submerged fermentation. Biotechnology and Bioengineering. 1998;57(4):409–419.

42. Thomen P et al. Bacterial biofilm under flow: first a physical struggle to stay, then a matter of breathing. PLOS One. 2017;12(4):e0175197. https://doi.org/10.1371/journal.pone.0175197

43. Hendrix RHJ, Ganushchak YM, Weerwind PW. Contemporary oxygenator design: shear stress-related oxygen and carbon dioxide transfer. Artificial Organs. 2018;42(6):611–619. https://doi.org/10.1111/aor.13084

44. Camacho E, Casadevall A. Cryptococcal traits mediating adherence to biotic and abiotic surfaces. Journal of Fungi. 2018;4(3):88.

45. Gonçalves AP et al. Allorecognition upon fungal cell-cell contact determines social cooperation and impacts the acquisition of multicellularity. Current Biology. 2019;29(18):3006–3017.

46. Miyazawa K, Umeyama T, Hoshino Y, Abe K, Miyazaki Y. Quantitative monitoring of mycelial growth of *Aspergillus fumigatus* in liquid culture by optical density. Microbiology Spectrum. 2022;10(1):e00063-21.

47. Miyazawa K, Umeyama T, Yoshimi A, Abe K, Miyazaki Y. Aspergillus cell surface structural analysis and its applications to industrial and medical use. Medical Mycology Journal. 2024;65(3):75–82.

48. Miyazawa K, Yoshimi A, Abe K. The mechanisms of hyphal pellet formation mediated by polysaccharides, α-1, 3-glucan and galactosaminogalactan, in Aspergillus species. Fungal Biology and Biotechnology. 2020;7(1):10.

49. Miyazawa K et al. Both galactosaminogalactan and α-1, 3-glucan contribute to aggregation of *Aspergillus oryzae* hyphae in liquid culture. Frontiers in Microbiology. 2019;10:2090.

50. Glass NL, Rasmussen C, Roca MG, Read ND. Hyphal homing, fusion and mycelial interconnectedness. Trends in Microbiology. 2004;12(3):135–141.

51. Read ND, Fleißner A, Roca MG, Glass NL. Hyphal fusion. Cellular and Molecular Biology of Filamentous Fungi. 2010:260–273.

52. Read ND, Lichius A, Shoji JY, Goryachev AB. Self-signalling and self-fusion in filamentous fungi. Current Opinion in Microbiology. 2009;12(6):608–615.

53. Wimpenny J, Manz W, Szewzyk U. Heterogeneity in biofilms. FEMS Microbiology Reviews. 2000;24(5):661–671. https://doi.org/10.1111/j.1574-6976.2000.tb00565.x

54. Palmer JG, Murmanis L, Highley TL. Visualization of hyphal sheath in wood-decay hymenomycetes. I. Brown-rotters. Mycologia. 1983;75(6):995–1004. https://doi.org/10.1080/00275514.1983.12023785

55. Palmer JG, Murmanis L, Highley TL. Visualization of hyphal sheath in wood-decay hymenomycetes. II. White-rotters. Mycologia. 1983;75(6):1005–1010. https://doi.org/10.1080/00275514.1983.12023786

56. González-Ramírez AI, Ramírez-Granillo A, Medina-Canales MG, Rodríguez-Tovar AV, Martínez-Rivera MA. Analysis and description of the stages of Aspergillus fumigatus biofilm formation using scanning electron microscopy. BMC Microbiology. 2016;16(1):243. https://doi.org/10.1186/s12866-016-0859-4

57. Gutiérrez A, Martínez MJ, Almendros G, González-Vila FJ, Martínez AT. Hyphal-sheath polysaccharides in fungal deterioration. Science of The Total Environment. 1995;167(1):315–328. https://doi.org/10.1016/0048-9697(95)04592-O

58. Moore D, McNulty LJ, Meskauskas A. Branching in fungal hyphae and fungal tissues: growing mycelia in a desktop computer. In: Branching Morphogenesis. Springer; 2005. p. 75–90.

59. Riquelme M et al. Fungal morphogenesis, from the polarized growth of hyphae to complex reproduction and infection structures. Microbiology and Molecular Biology Reviews. 2018;82(2):e00068-17. https://doi.org/10.1128/mmbr.00068-17

60. Shinde B, Khan S, Muhuri S. Model for growth and morphology of fungal mycelium. Physical Review Research. 2020;2(2):023111.

List of Symbols, Abbreviations, and Acronyms

ATCC	American Type Culture Collection
DI	Deionized
EPS	Extracellular Polysaccharides
PDA	Potato Dextrose Agar
YPD	Yeast Peptone Dextrose

1 (PDF)	DEFENSE TECHNICAL INFORMATION CTR DTIC OCA
1 (PDF)	DEVCOM ARL FCDD RLB CB TECH LIB